Journal of ELECTRONIC MATERIALS, Vol. 35, No. 10, 2006

Regular Issue Paper

Intergrowth Mechanism of Silicon Nanowires and Silver Dendrites

T. QIU,[1,2] X.L. WU,[1,2,3] G.G. SIU,[2] and PAUL K. CHU[2,4]

1.—National Laboratory of Solid State Microstructures and Department of Physics, Nanjing University, Nanjing 210093, People's Republic of China. 2.—Department of Physics & Materials Science, City University of Hong Kong, Kowloon, Hong Kong, People's Republic of China. 3.—E-mail: hkxlwu@nju.edu.cn. 4.—E-mail: paul.chu@cityu.edu.hk.

The intergrowth mechanism of silicon nanowires and silver dendrites formed by electroless metal deposition has been investigated by scanning electron microscopy. A self-assembled localized microscopic electrochemical cell model can adequately describe the self-organized Si nanowires growth. Using these in situ prepared Si nanowire arrays as templates, a diffusion-limited aggregation process is proposed to explain the formation of the silver dendritic nanostructures.

Key words: Nanoscale, electrochemical synthesis, morphology

INTRODUCTION

In the past, a variety of silicon nanostructures has been extensively studied.[1,2] Among them, silicon nanowires (SiNWs) have attracted considerable attention due to their potential applications in interconnects and basic components in future nanoelectronic and, especially, optoelectronic devices.[3–6] It has been suggested that SiNWs smaller than 100 nm in diameter may be used in high-speed quantum-wire field effect transistors and light-emitting devices with extremely low power consumption.[7]

A number of techniques based on the vapor-liquid-solid growth mechanism[8] have been developed to fabricate SiNWs, including physical vapor deposition, laser ablation, evaporation, and solution methods.[9–13] However, high temperature, hazardous silicon precursors, complex equipment, and other rigorous conditions are often the disadvantages of these techniques. Recently, a relatively fast and effective method has been developed to fabricate SiNWs.[6,14] This method is derived from electroless metal deposition on a silicon wafer and selective etching. Electroless metal deposition in an ionic metal (silver) HF solution is based on a microelectrochemical redox reaction in which both the anodic and cathodic processes occur simultaneously on the silicon surface.[15] This is a simple and inexpensive fabrication technique and has been widely used in the microelectronics and metal coating industries.[16–18]

Using this promising technique, we have previously assembled visible light-emitting semiconductor nanomaterials at the tips of SiNWs[19,20] resembling nano-beacons that are potentially useful in future nanodevices. However, the detailed growth process of the SiNWs is not clear due to the lack of direct experimental verification so far. Herein, we analyze the growth processes of large-area SiNWs and dendritic silver nanostructures in detail, using serially acquired scanning electron micrographs, and propose an intergrowth mechanism to explain the formation. Because the performance of silver in applications such as electronics, catalysis, and photonics can be significantly enhanced by forming silver nanostructures with well-controlled dimensions,[21,22] silver nanostructures that possess symmetrical and sharp silver dendrites that grow simultaneously bode well for these applications.

EXPERIMENTAL

First, *p*-type, B-doped silicon (100) (1–5 Ω cm) wafers were cleaned by acetone to degrease the Si surface, followed by etching in a diluted aqueous HF (~10 wt.%) solution for 10 min. Subsequently, the cleaned silicon wafers were etched in a 5.0 mol/L HF solution containing 0.02 mol/L silver nitrate at 50°C for different periods of time. The container is a conventional Teflon-coated stainless steel vessel. After the etching process, the silicon wafers were rinsed with de-ionized water and blown dry by air. The thick silver dendrites covering the silicon wafer were detached before microstructural investigation. Each etched silicon wafer was cut into two pieces. One piece was used as a control sample, and the other was treated in an ultrasonic water bath for a

(Received November 8, 2005; accepted May 22, 2006)

short time to clean the surface. The morphology and chemical composition of the samples were determined using a FEG JSM 6335 field-emission scanning electron microscope (SEM, JEOL Company, Tokyo, Japan) equipped with an EDAX PV7715/89 ME energy dispersive x-ray (EDX) spectrometer. All the measurements were performed at room temperature.

RESULTS AND DISCUSSION

Figure 1(a) shows the SEM image of surface morphology of the silicon wafer etched for 20 min. followed by a short-time (10 s) ultrasonic treatment. The diameters of the SiNWs can be observed to be in the range of 30–200 nm, and their lengths are 1–2 μm. It can be also found that some silver nanoclusters with diameters of 100–300 nm are still embedded in the Si nanowire array. The length of the SiNWs on the silicon wafer is observed to increase to ~7 μm after etching for 40 min. (see Fig. 1b). In comparison, the sample that undergoes ultrasonic treatment for a short time (10 s) shows no noticeable silver nanoclusters in the Si nanowire array. The observation is the same for the Si wafer after etching for 60 min.; that is, showing no silver nanoclusters in the array (see Fig. 1c). However, it can be observed that further increase in the silicon nanowire length (~25 μm) leads to tilting of the SiNWs, and the heads of some of the SiNWs are found to lean against each together.

The vapor-liquid-solid mechanism based on growth from a liquid metal seed particle[8] is generally accepted for the growth of one-dimensional (1D) silicon nanostructures. However, we believe that the formation mechanism of these as-synthesized SiNWs is quite different from the previously proposed mechanisms.[8,11,14] For the silver/silver ion system with a highly positive equilibrium potential [$E^{\circ}(Ag^{+}/Ag) = 0.7996$ V],[23] the energy levels of the silver ion overlap with those of silicon around the valence band, and silver deposition can occur on both *p*-type and *n*-type silicon in the dark via the injection of holes from the silver ion into the solution.[24–27] Figure 2 shows the schematic of the silver/silver ion system in which the acceptor states overlap the valence band of the silicon. For a *p*-type silicon, the injected holes can either be transported to the external circuit giving rise to a direct current, or they can be involved in an oxidation process such as etching of the silicon.[28] For *n*-type silicon, holes can recombine with electrons in the conduction band, resulting in a deposition current (if band bending is not too large), or under conditions of deep depletion, the holes can also be involved in an oxidation process.[28] If the positions of the band edges remain fixed during the deposition process, then if the reverse reaction is neglected, the deposition current is independent of the applied potential.

In the etching process, the holes injected from the silver ion are consumed by an oxidation process, and deposition can occur without an externally applied bias. The possible mechanisms for zero-current electroless deposition are shown in Fig. 3:

- The injected holes are consumed by oxidation on the silicon surface so that the substrate atoms are replaced by silver atoms (displacement plating).
- The holes injected during silver deposition are transferred to an electron donor in the solution.

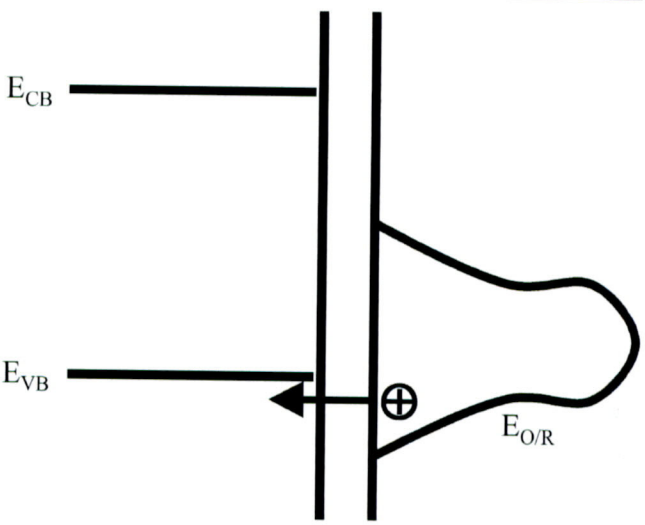

Fig. 2. Energy band diagram illustrating the possible mechanism for the deposition of silver onto silicon in contact with a solution, based on injection of holes into the valence band from the silver/silver ion system with a sufficiently positive equilibrium potential.

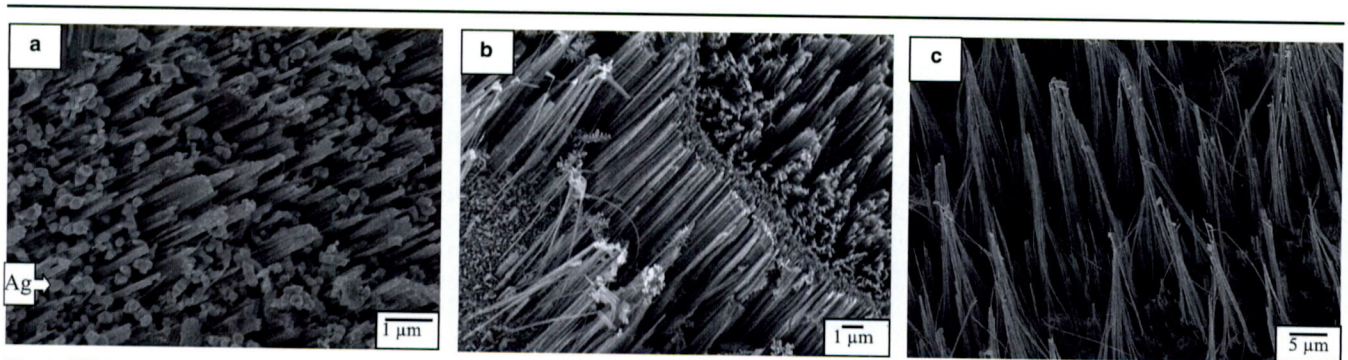

Fig. 1. SEM images of the silicon wafers etched for different times in a 5.0 mol/L HF solution containing 0.02 mol/L silver nitrate at 50°C, followed by a short-time ultrasonic treatment for (a) 20 min., (b) 40 min., and (c) 60 min.

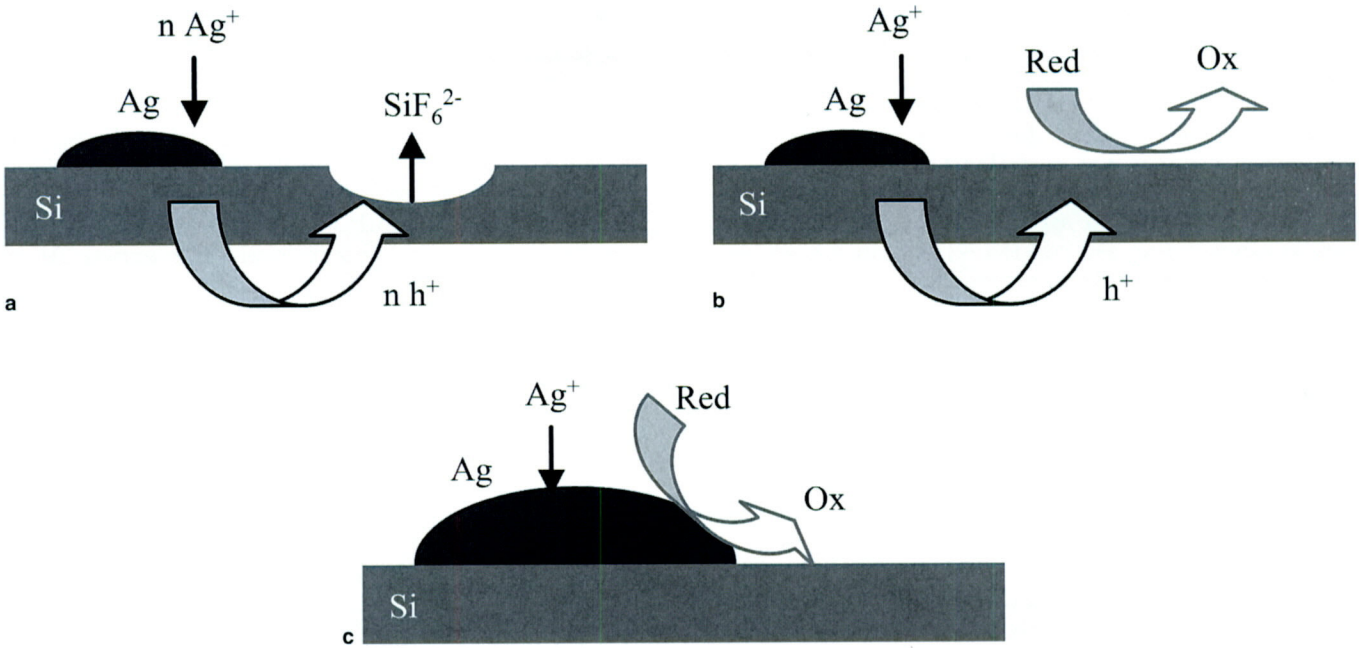

Fig. 3. Schematic illustrations of the three mechanisms of electroless deposition: (a) holes injected from silver ions (Ag^+) are consumed by silicon oxidation, and because the products (SiF_6^{2-}) are soluble, dissolution of the silicon (displacement plating) occurs; (b) injected holes are captured by an electron donor in the solution; and (c) silver ions are catalytically reduced on an existing silver nucleus involving electrons donated by a reducing agent in the solution.

- The silver ion and reducing agent in the solution react directly at catalytic sites on the surface without involving the substrate in the charge transfer process.

In the first case (Fig. 3a), the oxidation products must be soluble in the solution in order to prevent the formation of a passivating layer. This is possible on Si because SiO_2 is soluble in a low-pH HF solution. In principle, the thickness of the silver film is limited because the deposition process cannot continue once complete coverage is achieved. The morphology and adhesion of the deposit may be poor caused by the simultaneous dissolution of silicon and deposition of silver. The second case (Fig. 3b) is not often encountered in the deposition of metals on semiconductors because the rate of transfer of holes to the solution is usually slower than the trapping of holes by surface atoms, which is the first step in the oxidation mechanism. This situation is similar to the stabilization of semiconductor surfaces under illumination in photoelectrochemical energy conversion.[29] The third case (Fig. 3c) is often used in electroless deposition of metals on semiconductors. For instance, small clusters of palladium or some other activating metals are deposited by the displacement mechanism (Fig. 3a), and then they act as catalytic sites for the reduction of the metal ions and oxidation of the reducing agent in the solution.

Formation of nanostructured SiNWs with unique shape can be understood on the basis of a self-assembled localized microscopic electrochemical cell model.[6] At the initial stage, silicon etching and silver deposition occur simultaneously on the Si wafer surface. The deposited silver atoms form nuclei first and then nanoclusters, which are uniformly distributed on the surface of the silicon wafer. These silver nanoclusters and the Si surrounding these silver nuclei can, respectively, act as local cathodes and anodes in the electrochemical redox reaction, which can be formulated as two half-cell reactions 1 and 2:

$$Ag^+ + e^- \rightarrow Ag \quad (1)$$

and

$$Si + 6F^- \rightarrow SiF_6^{2-} + 4e^- \quad (2)$$

That is to say, numerous nanometer-sized free-standing electrolytic cells could be spontaneously assembled on the surface of the silicon wafer in the aqueous HF solution. As silver is deposited, the surrounding silicon acting as the anode is etched away, while silver nanoclusters acting as the cathode are successfully preserved, and many of them are dispersed in the silicon nanowire array. Thus, the presence of these nanoscale electrolytic cells leads to selective etching of the silicon wafer.

In silver deposition, the etched silicon wafer is always covered by a layer of thick silver dendritic film, which is rather loose and can be easily detached from the surface of the silicon wafer. This thick and loose silver film should originate from reduction of silver nitrate on the silicon surface. The deposited silver atoms form nanoclusters and stick together. In Fig. 1a, we can clearly see that the silver nanoclusters are embedded in the Si nanowire array, but in Figs. 1b and 1c, no noticeable silver nanoclusters are observed in the nanowire array. This indicates that with increasing etching time, most of the silver nanoclusters diffuse along the pore channels onto

the nearby preformed silver seeds above the SiNWs, thereby decreasing the number of silver nanoclusters in the nanowire array.

In order to verify this process, we fabricated such an etched silicon wafer. The sample fabrication procedures are described as follows. After etching for 1 min. in the mixed solution, the silicon wafer was annealed at 600°C in air for 10 min. to obtain the dense silver film. The annealed silicon wafer was subsequently put into the same vessel and etched for 60 min. After etching, the silicon wafers were rinsed with deionized water and blown dry by air. Figure 4a shows the SEM image of the etched silicon wafer. No similar SiNWs are observed, but many silver nanoclusters resembling islands are observed on the silicon wafer surface. This result indicates that the dense silver film formed at 600°C annealing limits diffusion of the silver nanoclusters from the nanopores of the surface layer, thereby hindering the formation of the self-assembled localized microscopic electrochemical cell. Figure 4b displays another SEM image of the etched silicon wafer. We can see that some nanopores still exist on the surface layer (indicated by the dark arrow), but there are no silver nanoclusters on the walls of the nanochannels or in the nanopores. It can be inferred from the two SEM images that the formation of the nanopores is a precondition for the subsequent silicon nanowire growth. Initially, many small, flat honeycombs form around one tiny deposited silver nanocluster. In other words, numerous nanosized honeycomb-like anodes and silver atoms acting as the local cathode form an electrochemical cell. With increasing etching time, the honeycombs around the silver nanoclusters are etched further, and many of them combine to form one nanopore (see the black arrow in Fig. 4b). Finally, the silicon honeycombs around the silver nanoclusters acting as anodes are etched together, forming the SiNWs.

The diffusion process of the silver nanoclusters can also be observed on the control silicon wafers with no subsequent ultrasonic treatment. At the initial stage, the deposited silver atoms form nuclei first and then nanoclusters, which are distributed on the surface of the silicon wafer, as shown in Fig. 5a. The corresponding EDX spectrum in Fig. 5b provides direct proof. Figures 5c–5h show the SEM images of the silicon wafers etched for different times. In Figs. 5c and 5d, the silver nanoclusters can be seen in the silicon nanowire array. After etching for 30 min., changes are observed on the surface of the silicon wafer. Many silver nanoclusters diffuse and stick together on top of the SiNWs (see Fig. 5e). In the samples etched for 40 min. and 50 min., the silver dendritic nanostructures can be found, as shown in Figs. 5f and 5g. The deeper the silicon wafer is etched, the more the silver nanoclusters diffuse and stick. In the 60 min. etched sample, we can see symmetrical branches of silver dendrites on the surface (see Fig. 5h). Figure 5i shows the cross-sectional SEM image of a 40 min. etched silicon wafer. It can be observed that the SiNWs are nearly perfectly perpendicular to the surface of the silicon wafer and have a uniform distribution.

We have also etched a plasma-treated silicon wafer with a diamond-like carbon (DLC) surface film using the same experimental procedures.[30] Because the carbon film cannot be etched away, no SiNWs are observed, but a large number of silver nanoclusters form on the surface (see Fig. 6). The results further prove that the formation mechanism of the silver dendrites is in situ growth of the SiNWs.

The formation mechanism of these observed silver dendritic nanostructures is schematically illustrated in Fig. 7. At the beginning, silicon etching and silver deposition occur simultaneously on the silicon surface. These cells can self-assemble on the surface of the silicon wafer. The synchronized growth of silver dendrites should be considered within the framework of a diffusion-limited aggregation model,[31] which involves cluster formation by the adhesion of a particle via a random path to a

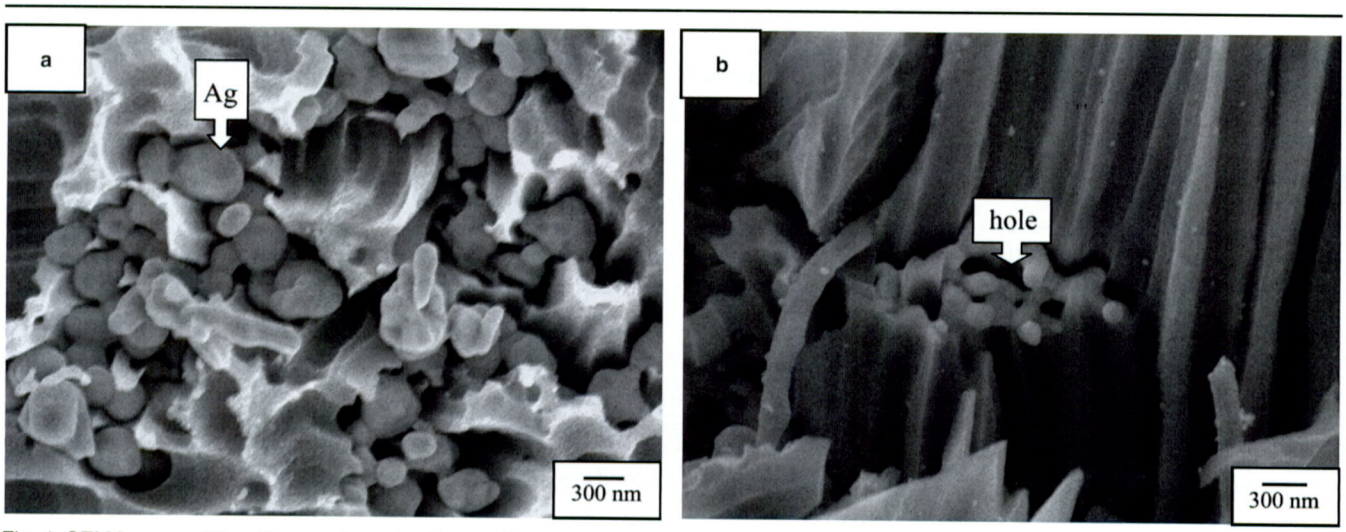

Fig. 4. SEM images of the silicon wafer etched by a different procedure, showing (a) many silver nanoclusters in the etched silicon wafer surface and (b) no silver nanoparticles in the nanopores.

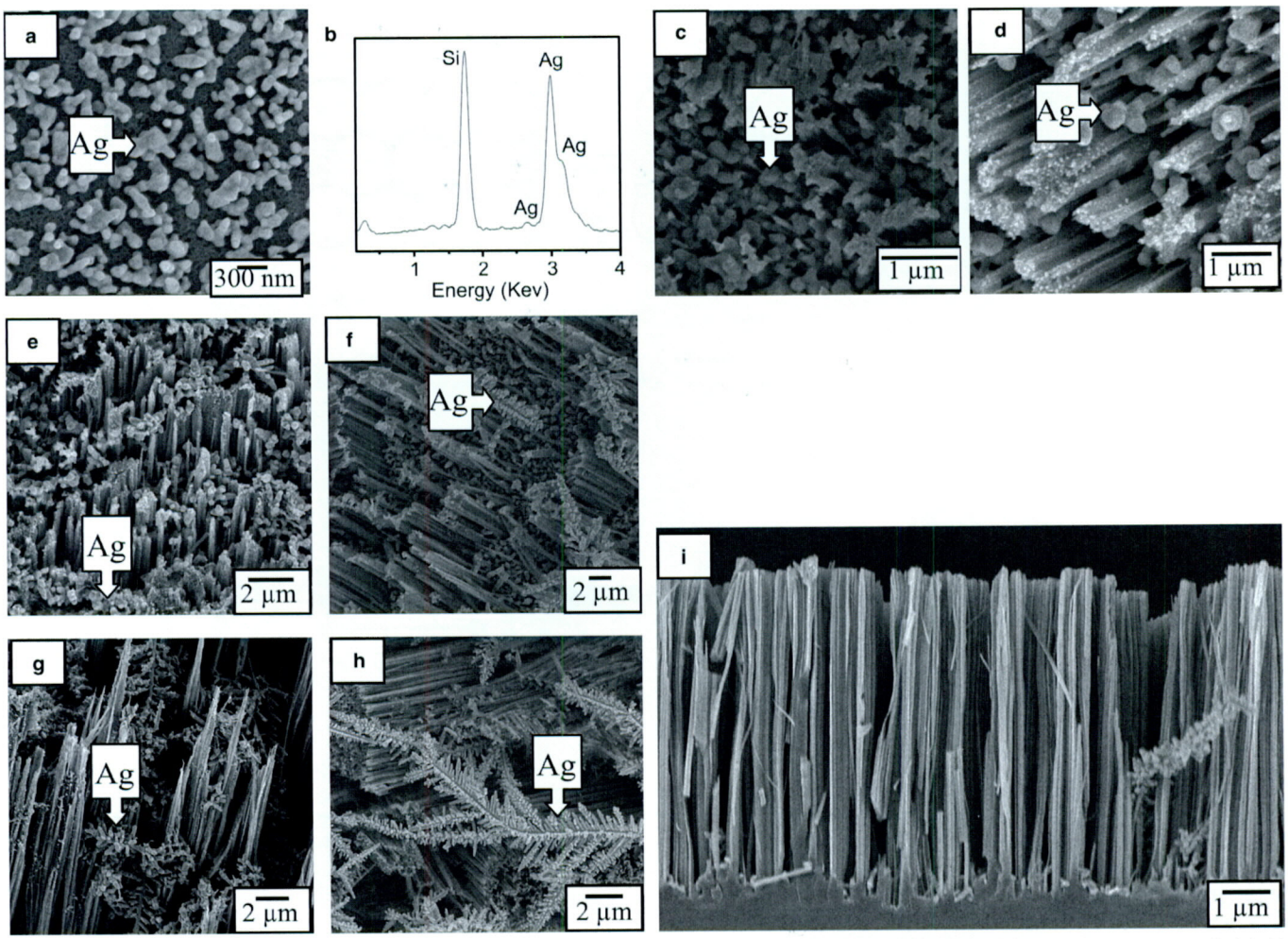

Fig. 5. SEM images of the silicon wafers etched for different times in a 5.0 mol/L HF solution containing 0.02 mol/L silver nitrate at 50°C: (a) 30 sec, (c) 10 min., (d) 20 min., (e) 30 min., (f) 40 min., (g) 50 min., and (h) 60 min. (b) EDX spectrum of deposited nanoclusters shown in 30 s etched silicon wafer. (i) Cross-sectional SEM image of 40 min. etched silicon wafer.

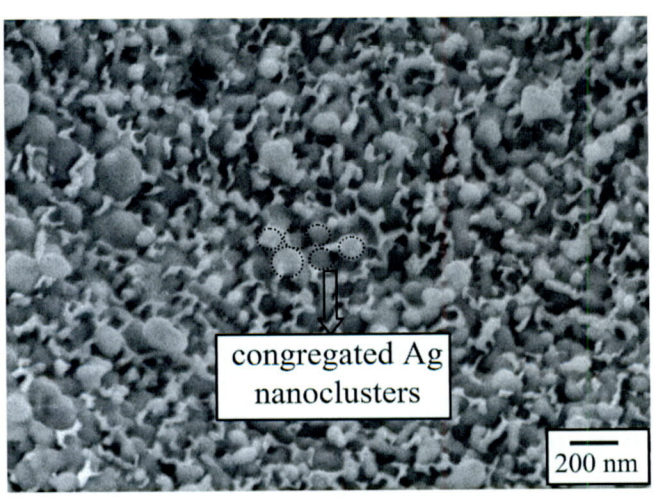

Fig. 6. SEM image of the silver film formed on the diamond-like carbon film.

selected seed on contact and allows the particle to diffuse and stick to the formed structure. The in situ prepared honeycombs around the silver nanoclusters can be regarded as the templates, similar to the work of Xiao on the synthesis of ultrasonically assisted template of palladium and silver dendritic nanostructures.[32] During the initial stage, a high concentration of the silver salt and reduction agent lead to reduction-nucleation-growth of the silver nanoclusters, forming a chain-like network. As the reaction continues, the concentrations of both the silver salt and reduction agent greatly decrease. The growth of silver nanoclusters is then mainly driven by the decreased surface energy resulting in the formation of the dendritic silver nanostructures.

CONCLUSIONS

The SiNWs and unique silver dendritic nanostructures have been self-organized via a simple electroless metal deposition method. Formation of the silver nanoclusters and SiNWs can be understood on the basis of the self-assembled localized microscopic electrochemical cell model. Using in situ prepared honeycombs around the silver nanoclusters as the templates, the synchronous growth of silver dendrites is considered within the framework of a diffusion-limited aggregation model. On

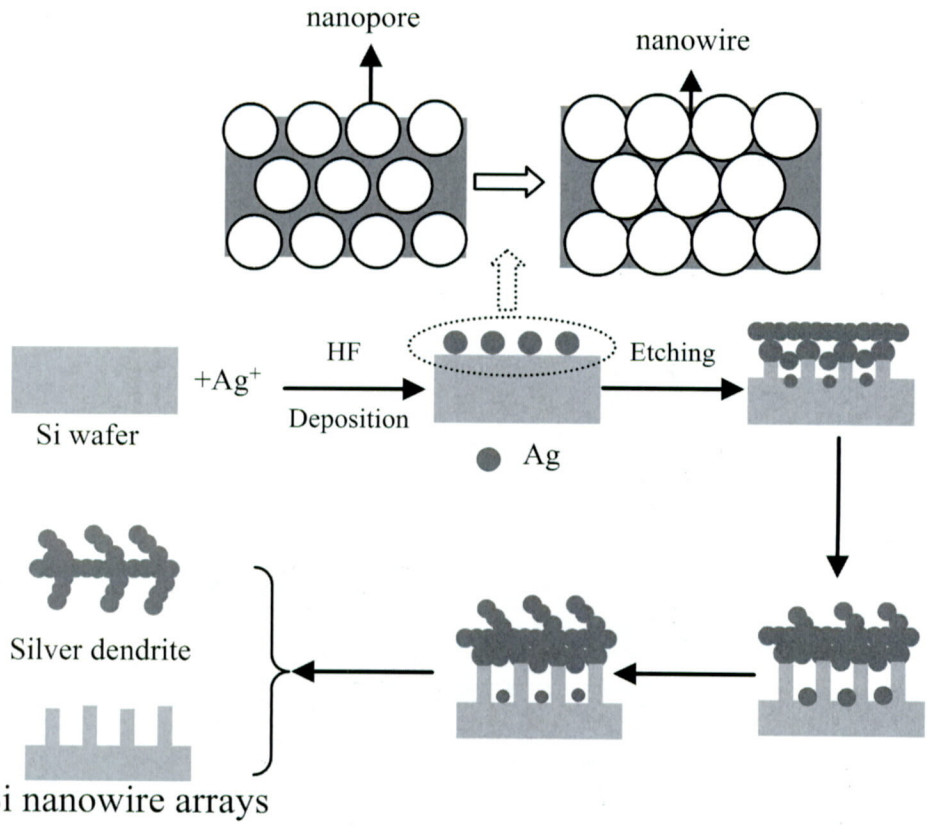

Fig. 7. Schematic illustration of the intergrowth process of the SiNWs and silver dendrites.

the basis of our proposed mechanism, we believe that the electroless metal deposition technique may also be extended to other metal/semiconductor systems, such as the formation of InP, SiC, and GaN 1D nanostructures.

ACKNOWLEDGEMENTS

This work was jointly supported by grants (10225416, 60476038, and 60576061) from the National Natural Science Foundations of China and City University of Hong Kong Direct Allocation Grant No. 9360110.

REFERENCES

1. J.T. Hu, O.Y. Min, P.D. Yang, and C.M. Lieber, *Nature* 399, 48 (1999).
2. U. Landman, R.N. Barnett, A.G. Scherbakov, and P. Avouris, *Phys. Rev. Lett.* 85, 1985 (2000).
3. Y. Cui and C.M. Lieber, *Science* 291, 851 (2001).
4. Y. Cui, Q.Q. Wei, H.K. Park, and C.M. Lieber, *Science* 293, 289 (2001).
5. M. Paulose, C.A. Grimes, O.K. Varghese, and E.C. Dickey, *Appl. Phys. Lett.* 81, 153 (2002).
6. T. Qiu, X.L. Wu, X. Yang, G.S. Huang, and Z.Y. Zhang, *Appl. Phys. Lett.* 84, 3867 (2004).
7. B. Marsen and K. Sattler, *Phys. Rev. B: Condens. Matter Mater. Phys.* 60, 11593 (1999).
8. R.S. Wagner and W.C. Ellis, *Appl. Phys. Lett.* 4, 89 (1964).
9. T.I. Kamins, R.S. Williams, Y. Chen, Y.J. Chang, and Y.A. Chang, *Appl. Phys. Lett.* 76, 562 (2000).
10. A.M. Morales and C.M. Lieber, *Science* 279, 208 (1998).
11. N. Wang, Y.F. Zhang, Y.H. Tang, C.S. Lee, and S.T. Lee, *Appl. Phys. Lett.* 73, 3902 (1998).
12. D.P. Yu et al., *Appl. Phys. Lett.* 72, 3458 (1998).
13. J.D. Holmes, K.P. Johnston, R.C. Doty, and B.A. Korgel, *Science* 287, 1471 (2000).
14. K.Q. Peng, Y.J. Yan, S.P. Gao, and J. Zhu, *Adv. Mater.* 14, 1164 (2002).
15. P. Gorostiza, M.A. Kulandainathan, R. Diaz, F. Sanz, P. Allongue, and J.R. Morante, *J. Electrochem. Soc.* 147, 1026 (2000).
16. C.H. Ting, M. Paunovic, P.L. Pai, and G. Chiu, *J. Electrochem. Soc.* 136, 462 (1989).
17. D.B. Wolfe, J.C. Love, K.E. Paul, M.L. Chabinyc, and G.M. Whitesides, *Appl. Phys. Lett.* 80, 2222 (2002).
18. A. Hilmi and J.H.T. Luong, *Anal. Chem.* 72, 4677 (2000).
19. T. Qiu, X.L. Wu, G.J. Wan, Y.F. Mei, G.G. Siu, and P.K. Chu, *Appl. Phys. Lett.* 86, 193111 (2005).
20. T. Qiu, X.L. Wu, Y.T. Xie, Y.F. Mei, G.G. Siu, and P.K. Chu, *Nanotechnology* 16, 2222 (2005).
21. I.R. Gould, J.R. Lenhard, A.A. Muenter, S.A. Godleski, and S.J. Farid, *J. Am. Chem. Soc.* 122, 11934 (2000).
22. Y.G. Sun and Y.N. Xia, *Adv. Mater.* 14, 833 (2002).
23. J.A. Dean, *Lange's Handbook of Chemistry,* 15th ed. (New York: McGraw-Hill, 1999).
24. A.J. Bard, R. Parsons, and J. Jordan, *Standard Potentials in Aqueous Solutions* (New York: Marcel Dekker, 1985).
25. M. Beltowska-Brzezinska, E. Dutkiewicz, and W. Lawicki, *J. Electroanal. Chem.* 99, 341 (1979).
26. H. Gerischer, *Physical Chemistry: An Advanced Treatise* (New York: Academic, 1970).
27. H. Gerischer, *Electrochim. Acta* 35, 1677 (1990).
28. G. Oskam, J.G. Long, A. Natarajan, and P.C. Searson, *J. Phys. D: Appl. Phys.* 31, 1927 (1998).
29. W.P. Gomes, S. Lingier, and D. Vanmaekelbergh, *J. Electroanal. Chem.* 269, 237 (1989).
30. R.K.Y. Fu, Y.F. Mei, L.R. Shen, G.G. Siu, P.K. Chu, W.Y. Cheung, and S.P. Wong, *Surf. Coat. Technol.* 186, 112 (2004).
31. T.A. Witten, Jr. and L.M. Sander, *Phys. Rev. Lett.* 47, 1400 (1981).
32. J.P. Xiao, Y. Xie, R. Tang, M. Chen, and X.B. Tian, *Adv. Mater.* 13, 1887 (2001).